Brain Stimulation 13 (2020) 753–764

Contents lists available at ScienceDirect

Brain Stimulation

journal homepage: http://www.journals.elsevier.com/brain-stimulation

Frequency-dependent electrical stimulation of fimbria-fornix preferentially affects the mesolimbic dopamine system or prefrontal cortex

Cornelia Helbing [a, b, *], Frank Angenstein [a, b, c, d, **]

[a] Functional Neuroimaging Group, Deutsches Zentrum für Neurodegenerative Erkrankungen (DZNE), Magdeburg, Germany
[b] Center for Behavioral Brain Sciences (CBBS), Otto von Guericke University, Magdeburg, Germany
[c] Leibniz Institute for Neurobiology (LIN), Magdeburg, Germany
[d] Medical Faculty, Otto von Guericke University, Magdeburg, Germany

ARTICLE INFO

Article history:
Received 14 November 2019
Received in revised form
6 February 2020
Accepted 19 February 2020
Available online 26 February 2020

Keywords:
BOLD fMRI
Fast-scan cyclic voltammetry
Nucleus accumbens
Hippocampus
Limbic system

ABSTRACT

Background: The fimbria/fornix fiber system is an essential part of the hippocampal-VTA loop, and therefore activities that are propagated through this fiber system control the activity of the mesolimbic dopamine system.
Objectives/hypothesis: We hypothesized that stimulation of the fimbria/fornix with an increasing number of electrical pulses would cause increasing activity of the mesolimbic dopamine system, which coincides with concurrent changes in neuronal activities in target regions of the mesolimbic dopaminergic system.
Methods: Right fimbria/fornix fibers were electrically stimulated with different pulse protocols. Stimulus-induced changes in neuronal activities were visualized with BOLD-fMRI, whereas stimulus-induced release of dopamine, as measured for the activity of the mesolimbic dopamine system, was determined in the nucleus accumbens with *in vivo* fast-scan cyclic voltammetry.
Results: Dependent on the protocol, electrical fimbria/fornix stimulation caused BOLD responses in various targets of the mesolimbic dopamine system. Stimulation in the low theta frequency range (5 Hz) triggered significant BOLD responses mainly in the hippocampal formation, infralimbic cortex, and septum. Stimulation in the beta frequency range (20 Hz) caused additional activation in the medial prefrontal cortex (mPFC), nucleus accumbens, striatum, and VTA. Stimulation in the high-gamma frequency range (100 Hz) caused further activation in the hippocampus proper and mPFC. The strong activation in the mPFC during 100 Hz stimulations depended not only on the number of pulses but also on the frequency. Thus, short bursts of 5 or 20 high-frequency pulses caused stronger activation in the mPFC than continuous 5 or 20 Hz pulses. In contrast, high-frequency burst fimbria/fornix stimulation did not further activate the mesolimbic dopamine system when compared to continuous 5 or 20 Hz pulse stimulation.
Conclusions: There exists a frequency-dependent dissociation between BOLD responses and activation of the dopaminergic system. Low frequencies were more efficient to activate the mesolimbic dopamine system, whereas high frequencies were more efficient to trigger BOLD responses in target regions of the mesolimbic dopamine system, particularly the mPFC.

Introduction

Deep brain stimulation (DBS; i.e., electrical stimulation of one central fiber bundle or one particular neuron population) has been proven as a suitable method to efficiently modify malfunctioning brain-wide neural networks. The mechanisms that eventually lead to altered brain-wide network activities are often complex and go beyond the simple activation/inhibition of a single neuron population. Effective DBS depends on specific physiological properties of targeted principal neurons, their actual interactions with local interneurons, and their control by different modulatory transmitter systems. When DBS is performed during functional magnetic

* Corresponding author. Deutsches Zentrum für Neurodegenerative Erkrankungen (DZNE), Leipziger Str. 44, 39118, Magdeburg, Germany.
** Corresponding author. Deutsches Zentrum für Neurodegenerative Erkrankungen (DZNE), Leipziger Str. 44, 39118, Magdeburg, Germany.
E-mail addresses: cornelia.hesse@dzne.de (C. Helbing), frank.angenstein@dzne.de (F. Angenstein).

https://doi.org/10.1016/j.brs.2020.02.026

resonance imaging (fMRI), affected brain-wide neuronal networks become detectable. Imaging studies in rodents, pigs, non-humans, and humans have demonstrated the efficacy of this technique in recent years [1–4].

Patients with chronic brain diseases such as depression, Parkinson's disease, dystonia, or Alzheimer's disease (AD) have already been successfully treated with the help of electrical DBS. For patients with AD, DBS of the fimbria/fornix system can improve disease symptoms like brain volume drop, memory loss, and memory retrieval [5,6]. AD is a neurodegenerative disease characterized by atrophy of several brain structures – notably, the hippocampus, temporal lobe, and parietal lobe – with amyloid and tau deposition [7–10] and impaired cerebral metabolism mostly in cortical regions [11]. These physiological changes result in dysfunction of several neural circuits including the default state network [12] and the memory circuit of Papez [13].

This so-called Papez circuit involves various structures of the brain [14]. It begins and ends with the hippocampal formation. Within this region, the hippocampus proper is crucial for episodic memory [15–17]. The fimbria/fornix system, another part of the Papez circuit, represents one major pathway of the limbic system and is primarily involved in the cortical control of consolidating and storing memory. Information is considered to flow within this circuit for a certain time and is linked to internal states (emotional and motivational modulation) before being processed for long-term storage.

Hippocampal efferents that originate in the CA1 and subiculum are bundled in the fimbria/fornix and project to the lateral septum, nucleus accumbens (NAcc), and different subdivisions of the prefrontal cortex and medial temporal lobe [18–21]. Furthermore, septal nuclei project via the fimbria/fornix system back to the hippocampus itself [22–24].

Either via the septum [19] and/or via mPFC-NAcc-ventral pallidum [25,26], the activity is also propagated to the ventral tegmental area (VTA). Thus, hippocampal activity also controls the activity of the mesolimbic dopamine system. In turn, intrahippocampal signal processing is modified by incoming activities from mesolimbic structures [27,28]. Thus, hippocampus and VTA form a loop (the so called hippocampal–VTA loop) that is required for the information flow into long-term memory and hippocampal-dependent learning [25,29].

Recent fMRI studies confirmed this close functional interaction between the hippocampal formation and the mesolimbic dopamine system. Thus, electrical stimulation of the perforant pathway, a major afferent fiber bundle to the dentate gyrus and hippocampus proper, generated significant BOLD responses in the VTA/substantia nigra region and, more importantly, triggered an increased dopamine release in the NAcc [30–32].

To further elucidate the mutual interaction between the hippocampal formation and the mesolimbic dopamine system, we stimulated the fimbria/fornix system, a hippocampal output structure, with 5 Hz (low theta rhythm), 20 Hz (beta rhythm), and bursts of 100 Hz (high gamma rhythm) pulses to search for optimal conditions to activate the mesolimbic dopamine system and to check its involvement in controlling brain-wide neuronal circuits that are triggered by different forms of hippocampal activity.

Material and methods

Animals

Animals were cared for and used according to a protocol approved by the Animal Experiment and Ethics Committee and in conformity with European conventions for the protection of vertebrate animals used for experimental purposes as well as institutional guidelines 86/609/CEE (November 24, 1986). The experiments were approved by the animal care committee of the state Saxony-Anhalt (No.: 42502-2-1218 DZNE) and performed according to the ARRIVE (Animal Research: Reporting In Vivo Experiments) guidelines. Male Wistar Han rats were housed individually under conditions of constant temperature (23 °C) and maintained on a controlled 12:12 h light:dark cycle with food and tap water ad libitum. For all *in vivo* experiments, 44 animals (MRI: n = 35, FSCV: n = 9) were measured. We used the minimum number of animals necessary to produce reliable scientific data.

Surgery & electrode implantation

In total, 44 adult male Wistar Han rats (8–9 weeks old, weighing 280–320 g) were used in this study. A stimulation electrode was implanted unilaterally in the hippocampal fimbria region using a rodent stereotaxic frame (Stoelting, Wood Dale, IL, USA). Each animal was anesthetized with Nembutal (40 mg/kg, i.p.) and placed in a stereotactic frame. The bipolar stimulation electrode (114 μm diamater, Teflon-coated tungsten wire, A-M systems, insulated except at the tip) was placed unilaterally in the right hippocampal fornical fimbria fiber tract (AP: 1.5 ML: 2.6 and DV: 2.5–3.3 from the dural surface) according to the rat atlas of Paxinos and Watson [33]. A monopolar recording was lowered into the right nucleus accumbens to adjust the correct placement of the stimulation electrode in the right FF fiber tract (AP: +1.7, ML: +1.6 and DV: 6.5–7.2 from dura). In addition, three holes were drilled into the skull, and plastic screws were placed to provide support in anchoring the electrode with dental acrylic (Paladur, Heraeus, Kulzer GmbH, Hanau, Germany). Both electrodes were fixed to the skull using dental acrylic.

Stimulation and data acquisition

Standard evoked pulse potentials were amplified and digitized with an interface (CED1401, Science Products GmbH, Hofheim, Germany) that was connected to and stored on a PC. To ensure the correct placement of the stimulation electrode, the averaged field potential was tested one week after surgery prior to the fMRI combined measurement. Standard stimulation experiments consisted of recording averaged field potentials in the NAcc evoked by FF-stimulation at low stimulus intensity (250 μA).

Electrical stimulation & functional MRI (fMRI)

All combined electrophysiology/fMRI measurements were performed on a 4.7T Bruker Biospec 47/20 animal scanner (free bore of 20 cm) equipped with BGA09 (400 mT/m) gradient system (Bruker BioSpin GmbH, Ettlingen, Germany. A 50 mm Litzcage small animal imaging system (Doty Scientific Inc., Columbus, SC, USA) was used for the RF signal reception.

All animals were initially anesthetized with isoflurane (1.5–1.8%; in 50:50 N_2:O_2; v:v), and the anesthesia was switched to deep sedation by application of medetomidine (Dorbene, Pfizer GmbH, bolus: 50 μg/kg s.c. and after 15 min 100 μg/kg per h s.c.) after animals were fixed into the head holder and connected to recording and stimulation electrodes.

All necessary MRI and electrophysiological adjustments for the simultaneous fMRI experiment were set in parallel before the measurement was started. Breathing, heart rate, and oxygen saturation were monitored throughout the experiment by an MRI-compatible pulse oxymeter (MouseOX™; Starr Life Sciences Corp., Pittsburgh, PA, USA). Heating was provided from the ventral site.

The pulse intensity for the fimbria stimulation protocol was always set to 250 μA. The pulse width was set at 100 μs The mode of stimulation was bipolar in all cases. The general stimulation protocol consisted of 10 consecutive stimulation trains given every minute after the 2-min baseline (Fig. 1). One stimulation train always lasted 8 s and was followed by a 52 s long stimulus-free interval. During one fMRI experiment the pulse pattern in each stimulation train was identical. In each fMRI experiment only one stimulation protocol was applied. If an animal was measured twice then the second measurement was not before 10 days after the first measurement.

The fimbria/fornix were stimulated by two different modalities; first by a continuous pulse sequence, i.e., continuous 5 Hz (low-frequent stimulation, theta), 20 Hz (beta), or 100 Hz (high-frequent stimulation, gamma) pulses during one stimulation train (i.e., 8s); second, by bursts of high frequency pulses, i.e., 5 or 20 pulses that were given every second during one stimulation train (i.e., 8 bursts during one stimulation train). Thus, during stimulation with continuous 5 Hz or bursts of 5 high-frequency pulses (and 20 Hz and bursts of 20 high frequency pulses, respectively) the number of pulses per train was identical, but the frequencies of these pulses were different (Fig. 1).

Imaging was performed as described previously [31]. For anatomical images, 10 horizontal T_2-weighted spin-echo images were obtained with a *RARE* sequence (rapid acquisition relaxation enhanced [34], using the following parameters: TR 4000 ms, TE 15 ms, slice thickness 0.8 mm, FOV 37 × 37 mm, matrix 256 × 256, RARE factor 8, and number of averages four. The total scanning time was 8 min 32 s. Functional MRI (fMRI) was performed with a gradient-echo EPI (echo planar imaging) sequence with the following parameters: TR 2000 ms, TE 24 ms, slice thickness 0.8 mm, FOV 37 × 37 mm, matrix 92 × 92, and total scanning time per frame 2 s. The slice geometry, i.e., ten horizontal slices, was identical to the previously obtained anatomical spin-echo-images.

Data processing and analysis

The functional data were loaded and converted to BrainVoyager data format. A standard sequence of pre-processing steps implemented in the BrainVoyager QX 2.8.0 software (Brain Innovation, Maastricht, the Netherlands) such as slice scan time correction, 3D motion correction (trilinear interpolation and reduced data using the first volume as a reference), and temporal filtering (FWHM 3 data points) were applied to each data set. Because the reconstruction of the fMRI images resulted in a 128 × 128 matrix (instead of the 92 × 92 imaging matrix), spatial smoothing (Gaussian filter of 1.4 voxel) was applied.

GLM analysis: Each individual functional data set was used for a multiple-subject GLM analysis implemented in BrainVoyager QX 2.8.0 software. Functional activation was analyzed by using the correlation of the observed BOLD signal intensity changes in each voxel with a predictor (hemodynamic response function) generated

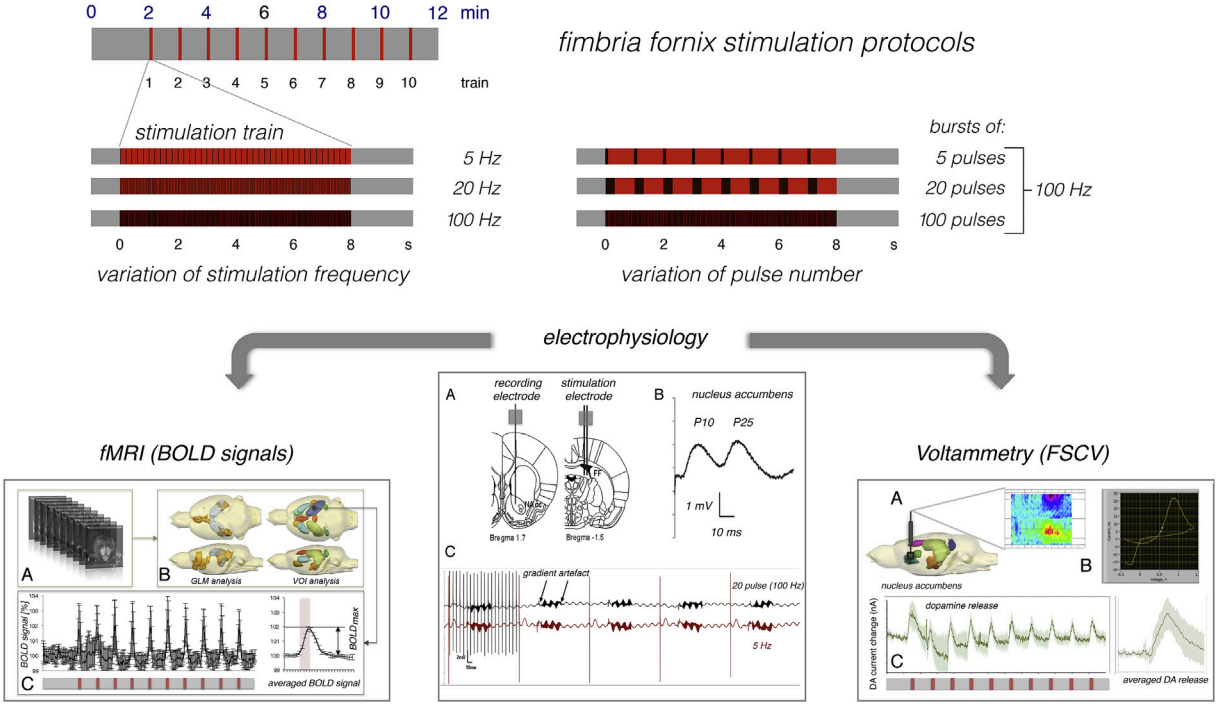

Fig. 1. Experimental setup to measure the effect of fimbria fornix stimulation. ***Top***: A general stimulation protocol was used for all fimbria-fornix stimulation experiments that consisted on 10 consecutive stimulation trains. Each stimulation train (indicated by red boxes) lasted 8s and was given every minute after the 2-min baseline. Fimbria-fornix fibers were stimulated either with different frequencies (left side) or with the same frequency (i.e., 100 Hz) but with different number of pulses per second (right side). Bottom: Fimbria-fornix stimulation was performed either in combination with BOLD-fMRI measurements (left panel) or with *in vivo* fast-scan cyclic voltammetry measurements (right panel). In vivo electrophysiological recordings of elicited neuronal responses in the nucleus accumbens always confirmed the correct location of electrodes (middle panel). ***fMRI measurements (left panel)***: Gradient-EPI images (**A**) were used for GLM analysis to detect all voxels that were significantly activated by the applied stimulus. In addition, volumes of interest (VOI) were marked **(B)**, and the average time course of all corresponding voxels were calculated and visualized as BOLD time series. Individual BOLD responses were averaged to depict an averaged BOLD response (**C**). ***Electrophysiological recordings (middle panel):*** **A**: scheme from a brain atlas [33] visualizing the target regions of implanted stimulation electrode in the hippocampal fimbria fibers and the recording electrode in the right nucleus accumbens (NAcc). **B**: electrophysiological signal that verified the right location of the stimulation electrode. **C**: electrophysiological recordings during the fMRI session. ***Measurements of dopamine release (right panel)*:** **A** For *in vivo* fast-scan cyclic voltammetry (FSCV) a carbon fiber electrode was implanted in the right nucleus accumbens. **B** FSCV recordings during one stimulation period. The cyclic voltammogram plot confirms the presence of dopamine. **C**: Variation of dopamine concentration during an entire stimulation experiment and the calculated average dopamine release during one stimulation period. (For interpretation of the references to color in this figure legend, the reader is referred to the Web version of this article.)

from the given stimulus protocol (see above). Based on this, the appropriate 3D activation map could be generated. To calculate the predictor, the square wave representing stimulus on and off conditions was convolved with a double gamma hemodynamic response function (onset 0 s, time to response peak 5 s, time to undershoot peak 15 s). To exclude false-positive voxels, a correction for serial correlation (csc) was performed (implemented in the BrainVoyager QX 2.8.0 software), and we considered only those with a significance level (p) above the threshold set by calculating the false discovery rate (FDR) with a q-value of 0.005 (which corresponds to a t-value greater than 3.8 or $p < 1.2 \times 10^{-4}$).

VOI analysis: Each individual functional imaging data set was aligned to a 3D standard rat brain using the 3D volume tool implemented in BrainVoyager QX 2.8.0 software. The following VOIs were marked in the 3D standard rat brain: right/left hippocampus (HC), right/left entorhinal cortex (EC), right/left nucleus accumbens (NAcc), right/left striatum, prefrontal cortex region, septum, right/left basolateral amygdala, right/left piriform cortex, and ventral tegmental area - substantia nigra (VTA-SN). The averaged BOLD time series of all voxels located in one VOI was then calculated for each individual animal using the volume-of-interest analysis tool implemented in the BrainVoyager QX 2.8.0 software. Each individual BOLD time series was normalized using the averaged BOLD signal intensity of 100%. Normalized BOLD time series were then averaged and depicted as mean BOLD time series ± SD. Based on the calculated BOLD time series, event-related BOLD responses were calculated by measuring the signal intensities starting six frames before stimulus onset (−12 s until 0 s), during stimulus presentation (between 0 s and 8 s, which corresponds to four frames), and the following 15 frames (8 s–38 s) after the end of the stimulus (Fig. 1). To avoid the confounding effect of putative variations in baseline BOLD signal intensities on the calculated BOLD response (i.e., BOLD signal $_{stimulus}$/BOLD signal $_{baseline}$ * 100%), each BOLD response was related to BOLD signal intensities of the stimulus over the preceding 12 s.

Significant changes in baseline BOLD signals were calculated as described previously [35] using paired t-tests. For each animal BOLD signal intensities measured between frame 6–58 (i.e., the period between 12 and 116 s) were averaged. These values were then compared to individual values at later time points. Significant stimulus-induced BOLD responses and differences in BOLD baseline signals were calculated using a two-sample equal variance *t*-test. Differences were considered significant at a calculated p-value < 0.05.

Fast-scan cyclic voltammetry

Fast-scan cyclic voltammetry (FSCV) was used to assess dopamine release in the rat NAcc during fimbria-fornix DBS. This assay was performed as previously described with a few modifications [31]. *In vivo* fast-scan cyclic voltammetry was performed with polymer-encased carbon fiber electrodes (7 μm diameter, ~100–150 μm length; Toray Carbon Fibers America, Inc., Santa Ana, CA, USA) as an acute procedure. The Ag/AgCl reference electrode was prepared from silver wires (0.5 mm diameter, Sigma-Aldrich, St Louis, MO, USA) chloridized in 0.1 M HCl. Extracellular dopamine was monitored at the carbon fiber electrode every 100 ms. All cyclic voltammograms were obtained with a triangular waveform (scan rate: 10 Hz, resting potential: −0.4 V, switching potential: 1.5 V, 400 V/s, 1000 samples per scan). Waveform generation and data collection were performed with the Invilog Voltammetric System and Software (Acquisition and Stimulation A&S, Invilog Research Ltd, Kuopio, Finland) and analyzed by a Fast Cyclic Voltammetry Analysis (FSV Analysis, Invilog Research Ltd, Kuopio, Finland) tool, which integrates FSCV and displays electrochemical measurements on a base station computer. The FSCV carbon fiber electrode was placed in the NAcc (AP: 1.7 mm, ML: 1.5 mm from bregma, DV: 6.6–7.3 mm from the dural surface).

Once the FSCV baseline was stable (less than 10% variation and no trending up or down across two successive recordings), electrical stimulation was performed in series (10 stimulation trains) starting after 2 min of baseline and given every minute for 8s. The applied pulses and stimulation pattern were identical to the stimulation protocols used for fMRI experiments. This was followed by a break of 30 min before starting the next stimulation paradigm with another 10 stimulation trains. Altogether, three FF-stimulation paradigms were presented to one animal.

Because of the inherent differences in sensitivity between Polymer-coated electrodes, *in vivo* changes in oxidation current recorded with different electrodes (in different animals) cannot be assumed to be equivalent. Thus, valid comparisons are possible only if the sensitivity of each electrode is calibrated against a standard and the electrochemical data are expressed as standard equivalent values. In the present study, DA was used as the standard to calibrate the working electrode sensitivity. Accordingly, *in vivo* changes in oxidation current are expressed as μM values of dopamine concentration. Therefore, the peak oxidation currents for dopamine in each voltammogram (at approximately 0.6 V) were converted into concentration from a post-experiment calibration against fresh solutions of 0.1–1 μM dopamine.

Statistical analysis

Animals with disconnected electrode implants were excluded from data analyses before the completion of the experiments. Data were analyzed using the Statistical Package for the Social Sciences 19.0 (SPSS, Chicago, IL) software with a two-tailed Mann-Whitney *U* test. If any of the main effects were significant, Tukey's *post-hoc* test was used for all comparisons unless otherwise specified. In all cases, $p < 0.05$ was set as the cutoff for statistical significance. A two-way ANOVA with repeated measures was used to evaluate the dopamine fluctuations during fast scan-cyclic voltammatry (FSCV).

Results

To describe how fimbria/fornix stimulation affects brain-wide neuronal networks, particularly the mesolimbic dopamine system, we performed two separate sets of experiments. First, we used fMRI to map stimulus-related BOLD responses in the entire brain, i.e. stimulus-related transient BOLD signal changes (BOLD response) as well as stimulus-related long-lasting variations in baseline BOLD signals [36]. Second, we performed FSCV to quantify the release of dopamine in one of the target regions of the VTA-SN, the nucleus accumbens (NAcc), during identical stimulation conditions. For each set of experiments, a different group of animals was used.

Electrical stimulation of fimbria-fornix with increasing pulse frequencies

The right fimbria/fornix was stimulated for short periods, and resultant BOLD signal variations in various brain regions as well as dopamine releases in the nucleus accumbens were monitored. The stimulation periods were kept identical (i.e., 8s), but the number of pulses varied. In a first set of experiments the fimbria/fornix were stimulated with different frequencies, thus, with continuous 5 Hz (40 pulses per train), 20 Hz (160 pulses per train), or 100 Hz (800 pulses per train) stimulation trains (Fig. 1).

Electrical stimulation with 5 Hz pulse trains (i.e., 40 pulses per train) elicited significant BOLD responses in several clusters that

cover parts of the right and left hippocampus (HC), right basolateral amygdala (BLA), the right and left entorhinal cortex (EC), the septum, the vertical limb of the diagonal bands of Broca (VDB), and the infra- and prelimbic cortex (PrL-IL, Fig. 2A). To characterize the activation in individual brain structures, we performed a volume-of interest (VOI) analysis (Fig. 2B).

Similar to perforant pathway stimulation [37], repetitive 5 Hz stimulation of the right fimbria/fornix system also elicited variable BOLD responses in the right hippocampus. A strong BOLD signal increase was induced during the first stimulation period. Then BOLD signals did not return to baseline level but remained elevated until the second stimulation period started. Only after the second stimulation period did BOLD signals rapidly decline significantly below the initial level. Starting with the fourth stimulation period, almost uniform BOLD responses were induced that were smaller than the first BOLD response (Fig. 2B, S1). The reduced baseline BOLD level persisted until the end of the experiment. The sustained elevation of BOLD signals after the first stimulation and the subsequent decline of baseline BOLD signals were observed in seven out of 10 animals. In the other three animals, the first stimulation period only caused a typical transient BOLD response with no subsequent significant decline in baseline BOLD signals (Fig. S2). The presence or absence of this sustained BOLD signal elevation after the first stimulation period also coincided with specific BOLD

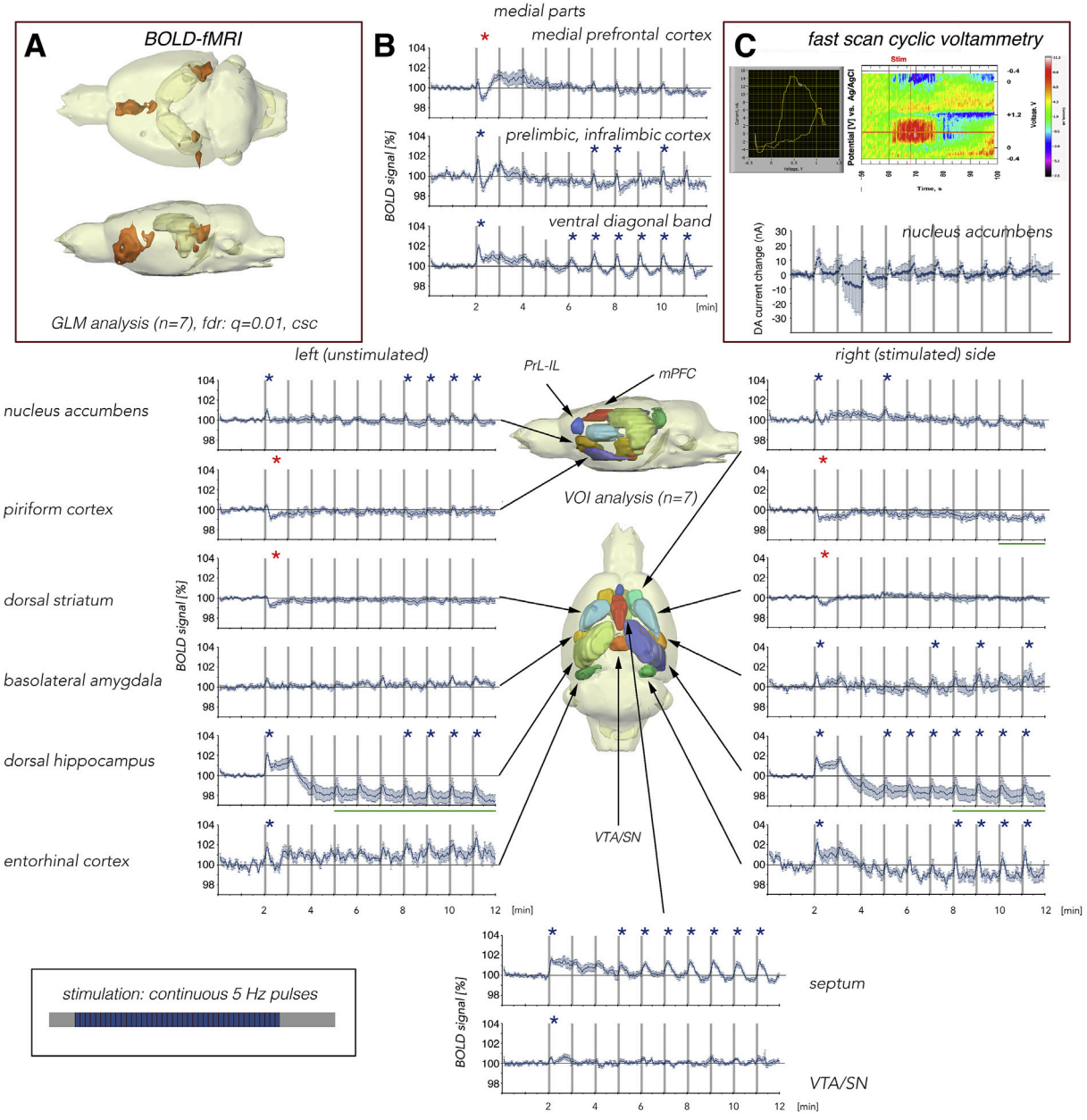

Fig. 2. Continuous 5 Hz pulse stimulation of the fimbria-fornix caused a regional-specific BOLD activation pattern as well as dopamine release in the nucleus accumbens. **A** Spatial distribution of significantly activated voxels in the rat brain. **B** Volume of interest analysis (VOI) revealed region-specific BOLD time series during repetitive electrical stimulations of the fright fimbria-fornix. Blue asterisks indicate stimulus-related significant positive BOLD responses and red asterisks indicate significant negative BOLD responses. Green lines indicate significantly declined baseline BOLD signals. **C** Upper part: Color-plot of dopamine efflux (dopamine oxidation at 0.6 V, dopamine reduction at −0.2 V) normalized to the average background current during two consecutive 5 Hz stimulation trains. Lower part: Time-dependent change in dopamine concentration in the nucleus accumbens during 10 repetitive stimulations of the fimbria fornix. (For interpretation of the references to color in this figure legend, the reader is referred to the Web version of this article.)

signal changes in other brain regions. Thus, only in the presence of these changes, a delayed transient negative BOLD response followed by a longer-lasting increase in BOLD signal was observed in the mPFC. A similar longer-lasting (3 min) increase in BOLD signal was observed in the VDB and septum, whereas in the VTA/SN region, only a short-lasting (1 min) increase occurred. (Fig. S2). In addition to these specific changes, 5 Hz pulse stimulation caused a delayed decrease in BOLD signal in the (left and right) piriform cortex and (left and right) dorsal striatum (Fig. S2) in all animals after the first stimulation period.

Stimulation of the fimbria/fornix system with 5 Hz pulse trains also resulted in a significant activation of the mesolimbic dopamine system as indicated by a stimulus-related increase in dopamine release into the right NAcc (Fig. 2C). Similar to stimulus induced BOLD responses in the NAcc, the first stimulation period caused the strongest dopamine release in the NAcc (Fig. S3).

Increasing the stimulation frequency to 20 Hz (i.e., 160 pulses per train) elicited significant BOLD responses in larger clusters (Fig. 3A, S4) when compared to 5 Hz stimulation trains.

VOI analysis revealed that the first stimulation period triggered positive BOLD responses in all regions that were activated by 5 Hz pulse stimulations (Fig. 3B). In contrast to 5 Hz pulse stimulation, 20 Hz pulse stimulation always caused in the hippocampus a sustained initial BOLD response with a subsequent persistent decline in baseline BOLD signal. The amplitude of the initial BOLD response in the right hippocampus was lower when compared to 5 Hz pulse stimulation but approximated during later stimulation trains (Fig. S1). Nevertheless, the concurrently induced initial BOLD responses in the piriform cortex, NAcc, BLA, EC, and mPFC were stronger than during 5 Hz pulse stimulation as well as during later stimulation trains (Fig. 3B, S1). Thus, 20 Hz pulse stimulation caused increased BOLD responses in several target regions of the hippocampal formation without affecting concurrent BOLD responses in the left and right hippocampus.

Increasing the stimulation frequency affected not only BOLD responses in various brain regions but also dopamine release in the right nucleus accumbens. Although the first stimulation period triggered a similar maximal dopamine release, the duration was prolonged, and eventually more dopamine was released. During subsequent stimulation trains, the maximal dopamine release was higher and the duration was longer (Figs. 2 and 3, S3). Thus, 20 Hz pulse stimulation was more efficient to activate the mesolimbic dopamine system than 5 Hz pulse stimulation.

A further increase in stimulation frequency from 20 to 100 Hz (i.e., 800 pulses per train) only caused a small increase in the cluster size of significantly activated voxels. An increase was found especially in the hippocampus and VTA/SN region (Fig. 4, S1, S4).

Using the VOI analysis to calculate the initial and later BOLD responses in the right hippocampus revealed again that the initial stimulation period elicited a sustained elevation of BOLD signal that declined after the second stimulation period until it reached a significantly lower level after the third stimulation period (Fig. 4B). Similar to repetitive 20 Hz pulse stimulation, this general decline in baseline BOLD signals was observed in all measured animals. In contrast to the 5 and 20 Hz pulse stimulation, individual BOLD responses to late stimulation trains were not reduced in comparison with the initial response. In contrast, the BOLD responses in the NAcc, dorsal striatum, PrL-IL, and VTA/SN were even stronger during late stimulation trains compared to the initial stimulation period (Fig. 4B, S1).

Increasing the stimulation frequency from 20 to 100 Hz did not further enhance the dopamine release in the NAcc, but caused a faster release. Thus during 100 Hz pulse stimulation maximal dopamine release was observed approximately 11s after onset of the stimulation, whereas during 20 Hz pulse stimulation the maximal dopamine concentration was measured after about 16 s (Fig. S3). Furthermore, during repetitive 100 Hz pulse stimulation dopamine release remained almost stable, except during the second stimulation period, when a reduced release was measured.

In summary, electrical stimulation of the fimbria/fornix with various frequencies resulted in a frequency-dependent BOLD activation pattern and quality of dopamine release. Repetitive 5 Hz pulse stimulation resulted initially in a strong activation of the right hippocampus, septum, VDB, and PrL-IL and a smaller activation during subsequent stimulation periods. In addition, the first 5 Hz pulse stimulation period caused a strong and delayed negative BOLD response in the mPFC that critically depended on the presence of concurrent elevated BOLD signals in the right hippocampus. A similar decline in BOLD signals was also present during 20 Hz pulse stimulation. However, because a stronger positive BOLD response was induced initially, the values did not drop below the initial baseline level. During 100 Hz pulse stimulation, this decline was not observed, although concurrent BOLD signals in the right hippocampus were also elevated. Repetitive 20 Hz pulse stimulation most efficiently generated BOLD responses in the right EC, right BLA, right piriform cortex, and mPFC, particularly during the initial stimulation period. In contrast, repetitive 100 Hz pulse stimulation most efficiently affected BOLD signals in the right NAcc, dorsal striatum, hippocampus, and VTA/SN during late stimulation trains.

During the first stimulation period, all three stimulation frequencies caused a similar increase of dopamine concentration in the NAcc. However, during 20 Hz and 100 Hz pulse stimulation, the increased dopamine concentration remained elevated longer. During subsequent stimulations, dopamine release declined during repetitive 5 Hz pulse stimulation but remained similar during 20 Hz or 100 Hz pulse stimulation. Thus, during repetitive stimulations, the 20 and 100 Hz pulse stimulation protocols were similarly effective to release dopamine in the NAcc, but the release occurred with different kinetics, i.e., fast during 100 Hz pulse stimulation and slightly delayed during 20 Hz pulse stimulation (Fig. S3).

Electrical stimulation of fimbria-fornix with increasing number of high-frequency pulses

In the first set of experiments, the fimbria/fornix was stimulated with different pulse frequencies during identical time periods, thus the stimulation frequency and the number of pulses varied. Therefore, observed differences could depend on the applied frequency (i.e., 5, 20, or 100 Hz) or simply on the number of applied pulses (i.e., 40, 160, 800). Therefore, we performed a second set of experiments in which the fimbria/fornix were always stimulated with 100 Hz pulses but with a different number of pulses, i.e., bursts of 5, 20, or 100 pulses per second (100 pulses corresponds to the continuous 100 Hz pulse stimulation).

As expected, with increasing the number of pulses per burst, cluster sizes of significantly activated voxels increased (Fig. S4). Similarly, dependent on the number of pulses, the amplitude of BOLD responses increased in many (but not all) brain regions. Thus, in the right piriform cortex, right BLA, and PrL-IL, bursts with 20 and 100 pulses caused similar BOLD responses, whereas in the right EC and mPFC, BOLD responses to 20 pulses even exceeded the responses to 100 pulses (Fig. 5, S5).

Measuring the stimulus-mediated dopamine release in the NAcc revealed a similar release during 5 and 20 pulse stimulation and a stronger release during 100 pulse stimulation. Thus, the strength of stimulus-induced BOLD responses and dopamine release did not match (Fig. 5).

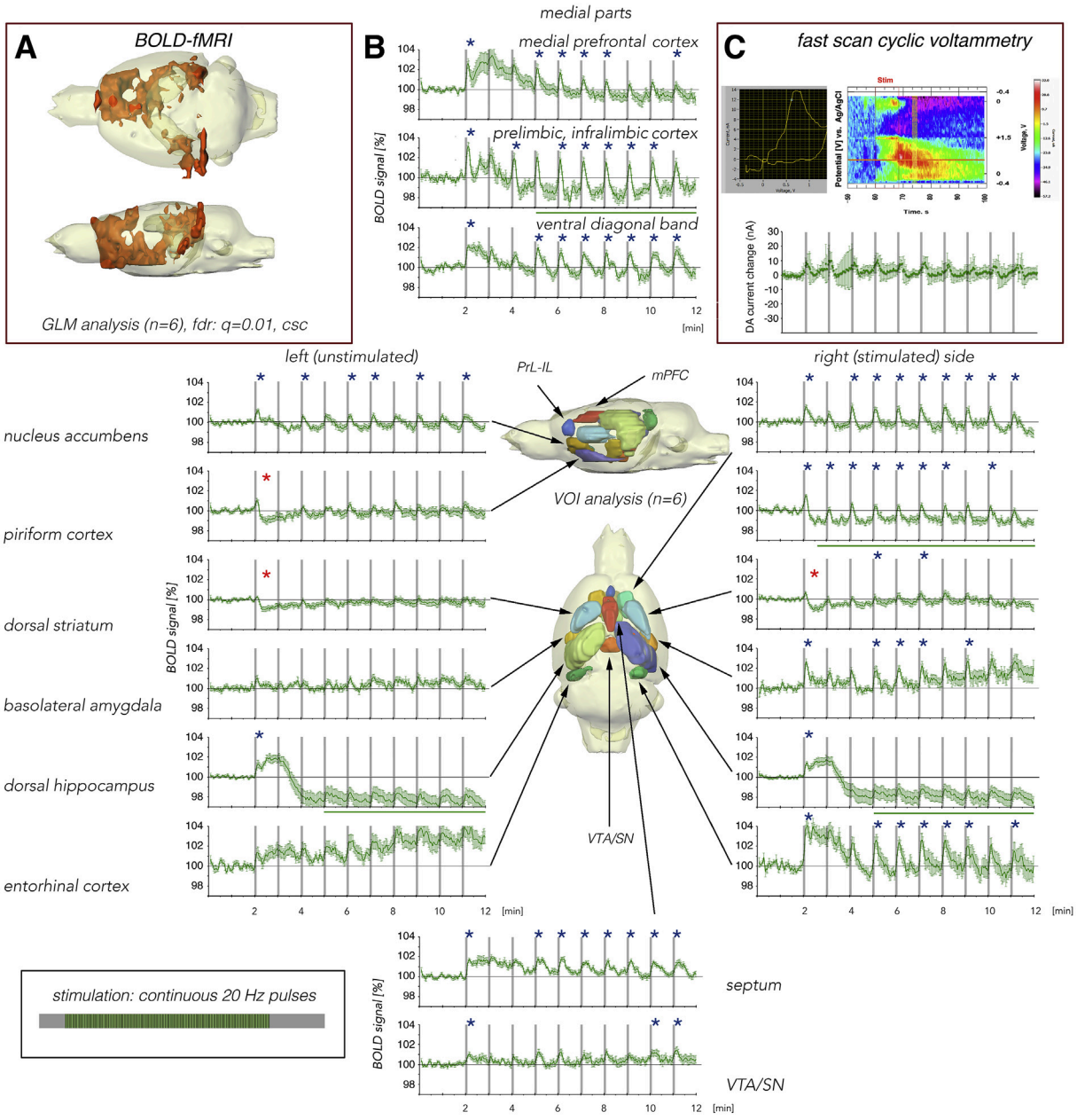

Fig. 3. Regional-specific BOLD activation pattern as well as dopamine release in the nucleus accumbens during continuous 20 Hz pulse stimulations of the fimbria-fornix. **A** Spatial distribution of significantly activated voxels in the rat brain. **B** Region-specific BOLD time series during repetitive electrical stimulations of the fright fimbria-fornix. **C** Corresponding dopamine release in the nucleus accumbens. Annotations: see Fig. 2.

Discussion

The primary purpose of the present study was to compare the efficacy of various fimbria/fornix stimulation protocols to activate the mesolimbic dopaminergic system. In this context, the current study confirms previous studies describing extensive projections of fimbria-fornix fibers to a variety of mesolimbic target areas [18,23,38–40] and extends these findings with the observation that the functional relevance of these connections critically depends on the applied frequency. As a parallel finding, *in vivo* FSCV confirmed previous findings that fimbria/fornix or ventral subiculum stimulation causes an activation of the mesolimbic dopamine system [41,42], and again this activation is frequency-specific. More importantly, stimulus-induced activation of the mesolimbic dopaminergic systems (as measured by the amount of dopamine release in the NAcc) was not mirrored by similar changes in BOLD responses in the VTA/SN region (the origin of dopaminergic projections) and/or target regions of the mesolimbic dopamine system, including the NAcc. This again agrees with previous findings that stimulus induced variations in BOLD signals can hardly be attributed to changes in dopamine release because there are mainly superposed by glutamatergic-mediated effects [30,31], although dopamine release has at higher field strength (≥7 T) a measurable effect on BOLD signals [43,44].

Frequency-dependent activation of different neuronal networks

Of particular interest is the observation that depending on the stimulation frequency, a different brain-wide neuronal network was activated. Raising the pulse frequency (i.e., from 5 to

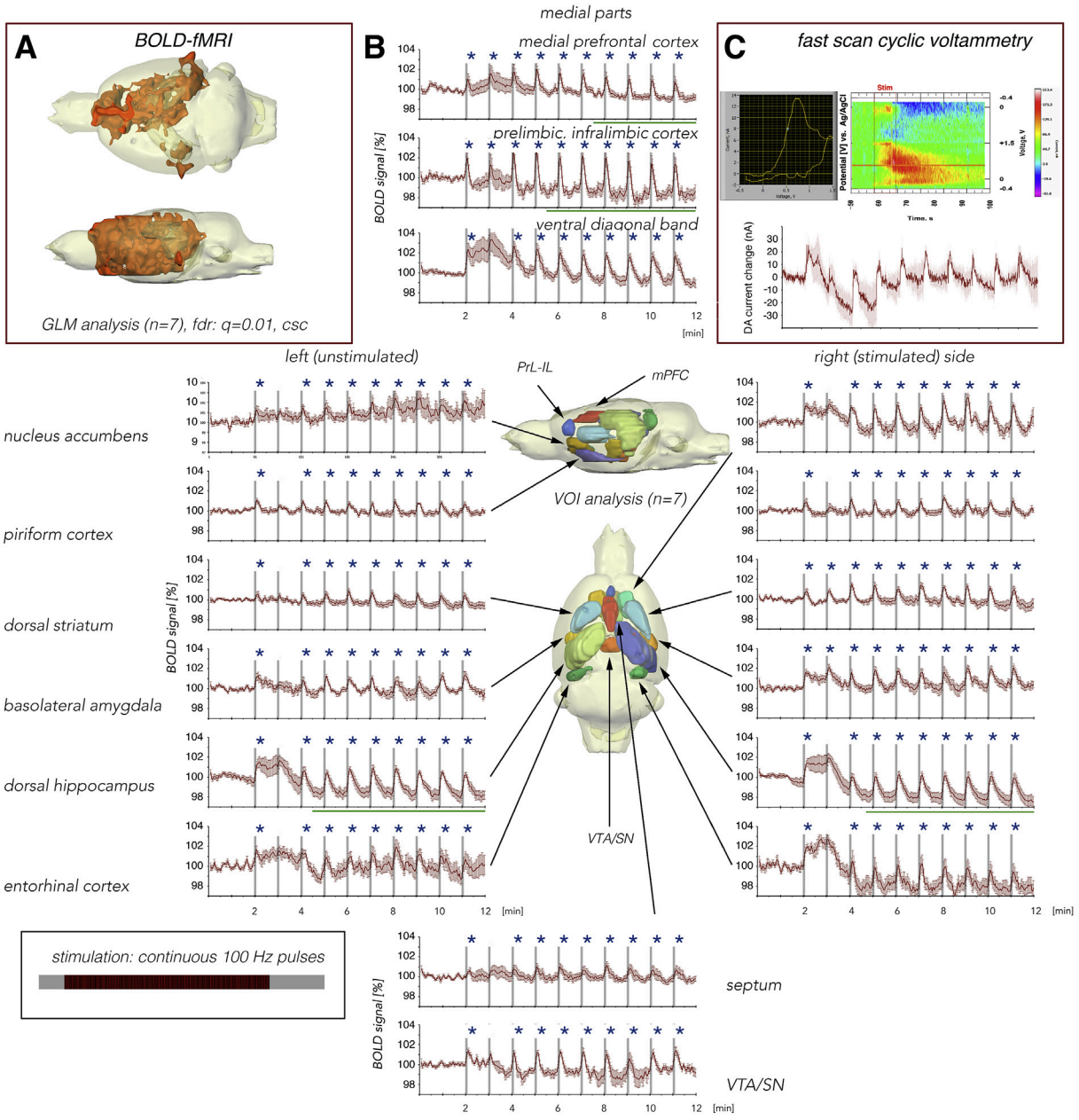

Fig. 4. Regional-specific BOLD activation pattern as well as dopamine release in the nucleus accumbens during continuous 100 Hz pulse stimulations of the fimbria-fornix. **A** Spatial distribution of significantly activated voxels in the rat brain. **B** Region-specific BOLD time series during repetitive electrical stimulations of the fright fimbria-fornix. **C** Corresponding dopamine release in the nucleus accumbens. Annotations: see Fig. 2.

20–100 Hz) caused stronger BOLD responses and spreading of significantly activated voxels (Fig. S4). However, no significant increase in dopamine release in the NAcc was found between continuous 20 and 100 Hz stimulation (Fig. 6, S3). These observations might depend on the applied frequency but also might be caused by the increasing number of applied electrical pulses per stimulus period (40, 160, or 800 per train). Applying different number of pulses with the same frequency also resulted in a spreading of significantly activated voxels (Fig. S4) but, interestingly, not always in stronger BOLD responses in individual brain regions (Fig. 5, S5). Thus, both stimulation frequency and number of pulses control the resultant BOLD response. The so far best evidence for a frequency-specific activation of brain-wide neuronal networks arises from a direct comparison of BOLD responses/dopamine releases during stimulation with the same number of pulses, which were applied either as high-frequency burst pulses or as continuous pulse sequence. First, stimulation of the fimbria/fornix with continuous 5 or 20 Hz pulses triggered significantly higher dopamine releases in the NAcc as the same number of pulses did when they were applied as high-frequency pulse bursts (Fig. 6A). Thus, continuous low frequency (i.e., 5 or 20 Hz) pulse stimulation of the fimbria/fornix was more effective to activate the mesolimbic dopamine system than stimulation with the same number of high-frequency pulses. On the other hand, high-frequency pulse burst stimulation of the fimbria fornix caused significantly stronger BOLD responses in the mPFC as the same number of pulses did when they were applied as a continuous pulse sequence. Thus, high-frequency stimulation is more effective to

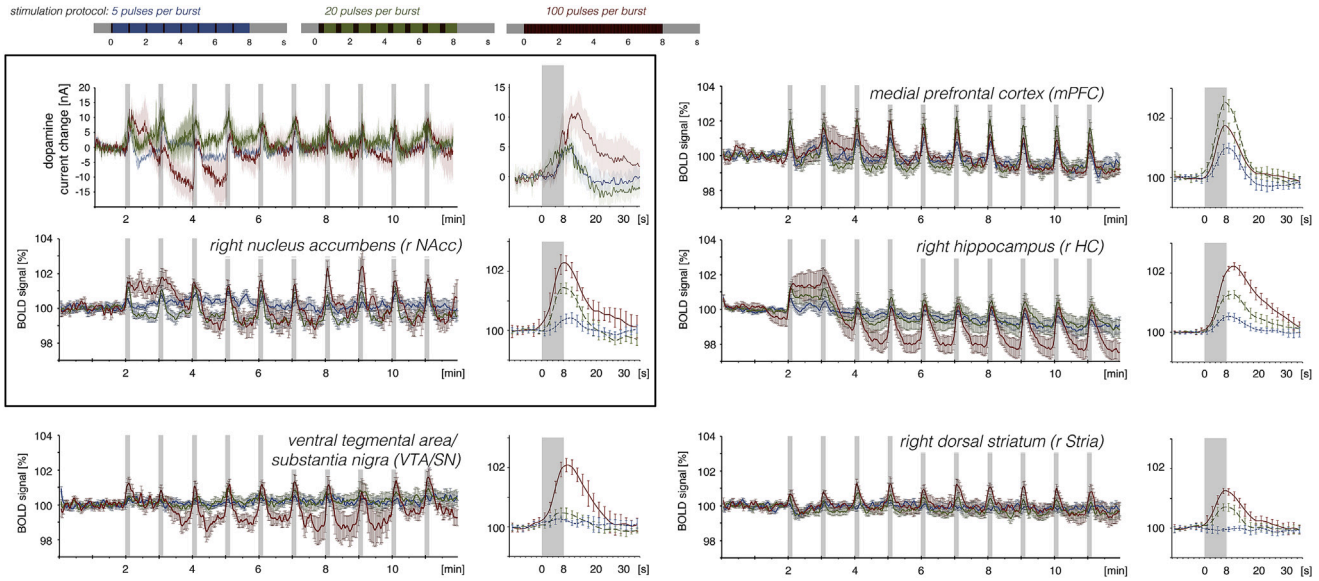

Fig. 5. Comparison of variations in dopamine concentration in the right nucleus accumbens and BOLD signal in various regions of the dopaminergic system during repetitive stimulations with different high-frequency pulse burst stimulation protocols. Blue dotted lines depict signals from stimulations with bursts of 5 pulses; green dotted lines depict signals measured during stimulations with bursts of 20 pulses and red lines from continuous 100 pulses. (For interpretation of the references to color in this figure legend, the reader is referred to the Web version of this article.)

generate BOLD responses in the prefrontal cortex (Fig. 6B). Moreover, the recorded hemodynamic response in the mPFC differed, i.e., the rising slope of the BOLD response to continuous 20 Hz pulse stimulation is delayed when compared to the rising slope of the BOLD response caused by bursts of 20 high-frequency pulses. This difference in the rising slope of the BOLD response was not present during the first stimulation period (Fig. 6B); it developed only after the initial stimulation. Variations in the initial slope of a hemodynamic response to an identical stimulus were previously observed in the hippocampus when an identical stimulus was applied under different anesthesia/sedation conditions [45] or when pair of pulses were applied with different inter-pulse intervals, which causes either a depression (20 ms) or facilitation (100 ms) of the second response [46]. Thus, the variation in the initial slope of the hemodynamic response in the mPFC might also reflect a different processing of the incoming pulses. Moreover, when BOLD time series from all analyzed brain regions were cross-correlated to reveal similar BOLD signal fluctuations as indicators for similar changes in neuronal activities, different functional connectivity maps emerged (Fig. 7). It is not certain whether these correlative BOLD signal changes represent synchronized neuronal activities, as long neuronal activities are not directly measured in these regions. However, these maps suggest that the mPFC interacts with more structures during high frequency pulse stimulations than during low frequency stimulations. Thus, whereas low frequency stimulation efficiently activates neuronal networks that eventually activate the mesolimbic dopamine system, the same pulse number applied as a high frequency pulse burst more efficiently activates neuronal network(s) that eventually activate the prefrontal cortex. In the context of using the fimbria/fornix as a target for deep brain stimulation (DBS), repetitive periods of low frequency pulse (between 5 and 20 Hz) should be used to enhance the activity of the mesolimbic dopamine system, whereas bursts of high-frequency pulses (100 Hz) might preferentially activate neuronal networks that affect functions in the mPFC.

Consecutive fimbria/fornix stimulation caused a sustained decline in baseline BOLD signals in the left and right dorsal hippocampus, which started after the third or forth stimulation period and persisted until the end of the experiment (Figs. 2–4). A similar decline of baseline BOLD signals in the hippocampus was previously observed during repetitive perforant pathway stimulations as soon as neuronal afterdischarges were induced [35]. Neuronal afterdischarges were normally elicited during or after the first stimulation period and coincided with a prolonged elevation of BOLD signals after the stimulation period [32]. In the present study, all used fimbria/fornix stimulation protocols could cause a sustained decline in baseline BOLD signals, thus it was not frequency dependent, it rather depended on the appearance of neuronal afterdischarges, as the prolonged elevation of BOLD signals after the first stimulation period indicate (Fig. S2). The neurophysiological basis for the significant decline is still not known, however it does not to depend on a general decrease of ongoing neuronal activity but rather on a changed activity of interneurons [35]. These findings agree with the recent finding of an *in vivo* electrophysiology study, that short unilateral electrical stimulation of the fornix with 40 Hz pulses elicited subsequently bursting activity in the hippocampus, which were followed by a sustained change in the local field potential (LFP) spectrum, i.e., short stimulation of fimbria/fornix fiber resulted in an altered network “state” in the hippocampus, which persisted for at least 12 min [47]. If the BOLD baseline shift is related to the stimulus-induced altered network “state” then short (consecutive) low frequency pulse stimulations are already sufficient to affect the network “state” of the hippocampus. This is of particular interest as fornix stimulation is also considered as target to treat epilepsy [48,49]. In this context, short low frequency and high-frequency pulse trains would effectively modify the network “state” of the hippocampus but high-frequency pulse trains would also modify brain wide neuronal networks that affect the mPFC, thus low frequency pulse protocols might be better suited to selectively modify hippocampal functions.

Stimulus-induced dopamine release vs. BOLD response

Dopamine is a complex neuromodulator, which is neither strictly excitatory nor strictly inhibitory but rather depends on the functional state of the target regions and its neurons [50]. As a major

source of dopamine, activity of the VTA/SN is supposed to be the first hint for dopamine release in the target region of the limbic system [51]. Midbrain dopamine neurons are located within the SN and VTA, which also contain GABAergic neurons and glutamatergic neurons. While the majority of neurons that project from the VTA to the NAcc are dopaminergic (about 65%), approximately a quarter (25%) of this population are GABAergic and 2–3% glutamatergic [52–58]. In a previous study, we found that BOLD responses in the mPFC that were induced by the same electrical stimulation paradigm were almost completely abolished in the presence of MK801 [31], which indicates that the elicited BOLD response largely depends on the activation of glutamatergic receptors. Indirect evidence suggests that the mesolimbic dopaminergic neurons release glutamate as a co-transmitter to communicate with target neurons in the forebrain [59]. However, the existence of glutamatergic signaling by DA neurons *in vivo* remains extremely controversial. Furthermore, selective activation of dopaminergic neurons in the VTA/SN by an optogenetic approach resulted in no significant BOLD responses in the mPFC or in any other mesolimbic target region, even though dopamine was released in the NAcc [30]. The results of the present study also indicate that it is not possible to unambiguously relate the strength of BOLD signals in the SN/VTA region as a region of origin for dopaminergic neurons or in various target regions of dopaminergic projections with the activity of the dopaminergic system. In general, when fimbria-fornix stimulation triggered significant BOLD responses in the SN/VTA region, dopamine releases in the NAcc were also observed. However, a dopamine release in the NAcc was also observed when no significant BOLD response was elicited in the SN/VTA region. Thus, the absence of significant BOLD responses in the SN/VTA during stimulation does not prove an inactive dopaminergic system. Furthermore, comparing the time series of dopamine concentrations in the NAcc and BOLD signals in the SN/VTA during repetitive stimulation with continuous 100 Hz pulses revealed different variations in the responses (Fig. S3). Thus, whereas the amount of dopamine release remained almost similar during all stimulation periods, BOLD responses significantly increased. Therefore, the strength of a BOLD response in the SN/VTA region is not related to the amount of dopamine release in the NAcc as one main target region of the dopaminergic system. Similarly, in all analyzed main target regions of the mesolimbic dopamine system (i.e., NAcc, mPFC hippocampus, PrL-IL or the mesostriatal dopamine system, i.e., dorsal striatum), the strength of BOLD responses did not match the amount of dopamine released in the NAcc as a marker for the activity of the dopaminergic system. Moreover, BOLD time series in these regions did not follow the BOLD time series of the VTA (Fig. 6C). All these observations indicate that BOLD-fMRI is not well suited to detect or monitor stimulus-induced changes in the activity of the dopaminergic system.

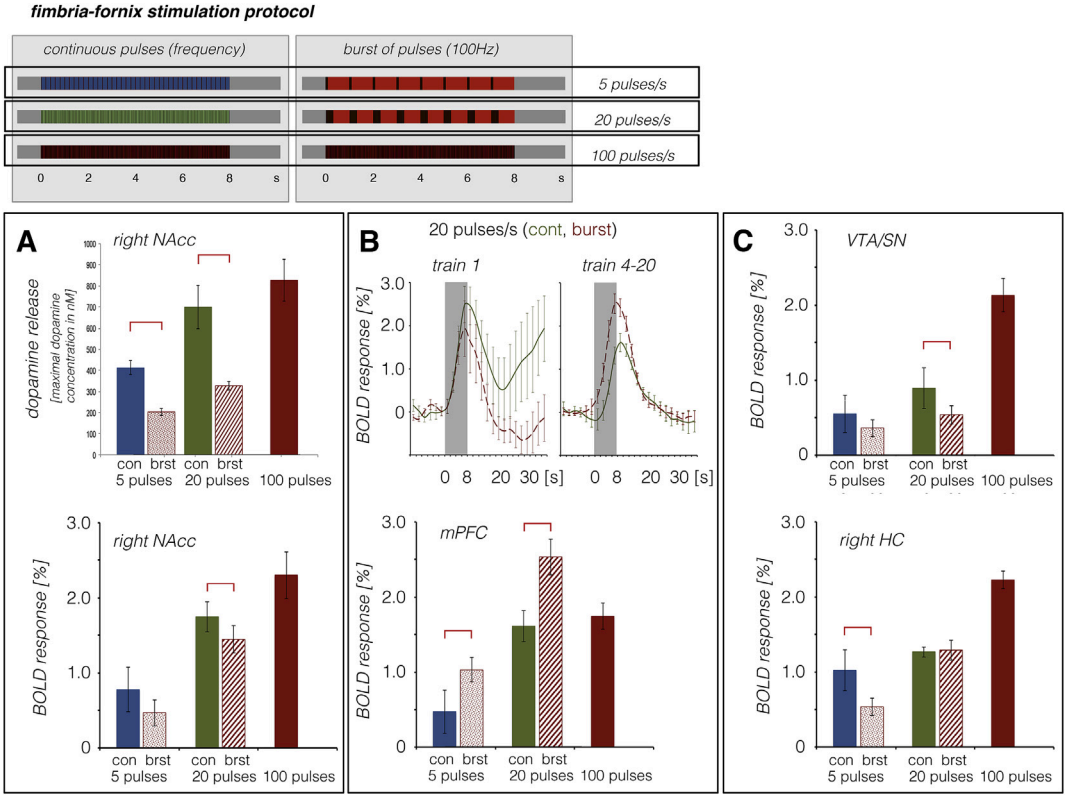

Fig. 6. Comparison of responses induced by identical number of pulses, which were applied with different pattern, i.e., as continuous pulse sequence or as bursts of high-frequency pulses (upper panel). **A** Fimbria-fornix stimulation with bursts of high-frequency pulses (brst, red colums, graphs) were less effective to release dopamine in the nucleus accumbens as the same number of pulses did when they were applied as continuous pulse sequence (con, 5 Hz -blue colums, green columns/graphs 20 Hz). Corresponding BOLD responses in the nucleus accumbens were only significantly different between the two 20 pulse stimulation protocols. **B** In contrast, fimbria-fornix stimulation with bursts of high-frequency pulses elicited significantly stronger BOLD responses in the mPFC as the same number of pulses did when they were applied as continuous pulse sequence. Whereas during continuous 20 Hz pulse stimulation BOLD responses declined after the first stimulation period, BOLD responses increased with repetitive stimulations when the pulses were applied as high-frequency pulse bursts. Note, that the onset of the initial slope of the hemodynamic response curve was similar during the first stimulation period but differed during subsequent stimulation periods. **C** Comparison of BOLD responses in the VTA and right hippocampus. Again, BOLD responses did not completely mirror the activity of the dopaminergic system as measured by the dopamine release. (For interpretation of the references to color in this figure legend, the reader is referred to the Web version of this article.)

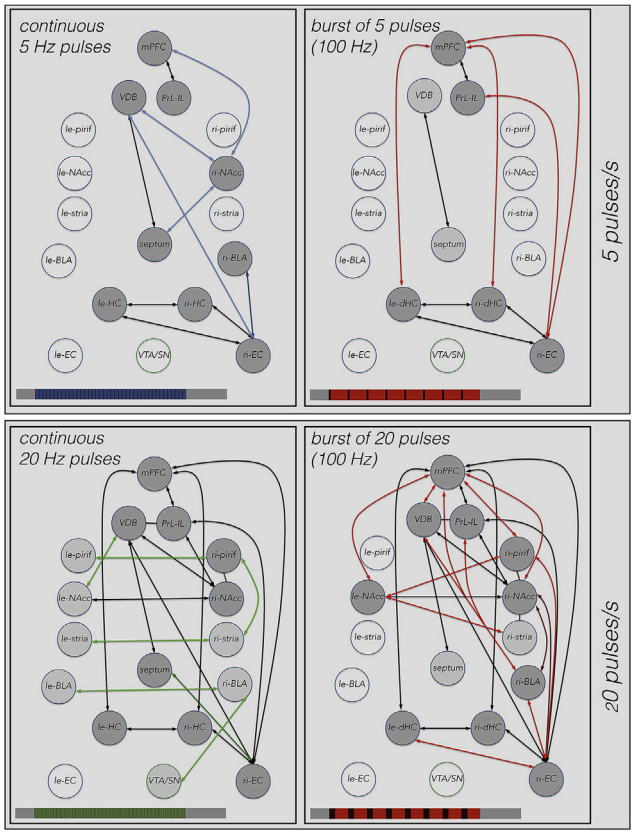

Fig. 7. Summary of regions with correlative BOLD time series (correlation coefficient r > 0.7) as indication for functional connectivity (fc). Regions with stimulus-induced significant activations are highlighted grey color. When the same number of pulses (5 pulses upper part, 20 pulses lower part) where applied as high-frequency pulse bursts then functional connectivity of the mPFC increased (black arrows: common fc, colored arrows: stimulation pattern specific fc). (For interpretation of the references to color in this figure legend, the reader is referred to the Web version of this article.)

Limitations

One limitation of the present study is that all animals were anesthetized or sedated during fMRI and FSCV sessions. Sedation is known to alter BOLD signal changes when compared to other forms of anesthesia [60] or awake animals [61]. General limitations of fMRI have been extensively discussed elsewhere [2], although several specific limitations are particularly pertinent to concurrent electrical stimulation.

Conclusion

Electrical stimulation of fimbria-fornix fibers activates different frequency-specific brain-wide neuronal networks. Whereas 5 and 20 Hz pulse stimulations are highly effective to activate the mesolimbic dopamine system, 100 Hz pulse stimulation efficiently activates brain-wide neuronal networks that include the mPFC. In the context of using the fimbria/fornix fibers as targets for deep brain stimulation to improve cognition or behavior in Alzheimer's disease [62–66], it should be noted that variations in stimulation frequencies might result in fundamentally different functional outcomes. Furthermore, no clear relations were found between stimulus-induced activation of the dopaminergic system and the corresponding BOLD response pattern, i.e., neither BOLD responses in the SN/VTA region, the origin of dopaminergic neurons, nor BOLD responses in main target regions of the dopaminergic system coincide with changes in measured dopamine release. Thus, unambiguous conclusions about stimulus-related changes in the activity of the dopaminergic system cannot be drawn from BOLD-fMRI measurements.

Declaration of competing interest

The authors confirm that there are no known conflicts of interest associated with this publication and there has been no financial support for this work that could have influenced its outcome.

CRediT authorship contribution statement

Cornelia Helbing: Conceptualization, Methodology, Investigation, Formal analysis, Writing - original draft, Funding acquisition. **Frank Angenstein:** Conceptualization, Methodology, Formal analysis, Writing - review & editing, Funding acquisition.

Acknowledgement

The authors wholeheartedly acknowledge Ms. Karla Krautwald for her assistance in the preparation of the animals as well as for her work in animal care and Dr. Jörg Stadler for the technical assistance. This project was supported by the CBBS-ScienceCampus founded by the Leibniz Association, SAS-2015-LIN-LWC.

Appendix A. Supplementary data

Supplementary data to this article can be found online at https://doi.org/10.1016/j.brs.2020.02.026.

References

[1] Angenstein F, Kammerer E, Scheich H. The BOLD response in the rat Hippocampus depends rather on local processing of signals than on the input or output activity. A combined functional MRI and electrophysiological study. J Neurosci 2009;29(8):2428–39.
[2] Logothetis NK. What we can do and what we cannot do with fMRI. Nature 2008;453(7197):869–78.
[3] Logothetis NK, Pauls J, Augath M, Trinath T, Oeltermann A. Neurophysiological investigation of the basis of the fMRI signal. Nature 2001;412(6843):150–7.
[4] Min HK, Hwang SC, Marsh MP, Kim I, Knight E, Striemer B, et al. Deep brain stimulation induces BOLD activation in motor and non-motor networks: an fMRI comparison study of STN and EN/GPi DBS in large animals. Neuroimage 2012;63(3):1408–20.
[5] Laxton AW, Tang-Wai DF, McAndrews MP, Zumsteg D, Wennberg R, Keren R, et al. A phase I trial of deep brain stimulation of memory circuits in Alzheimer's disease. Ann Neurol 2010;68(4):521–34.
[6] Lozano AM, Fosdick L, Chakravarty MM, Leoutsakos JM, Munro C, Oh E, et al. A phase II study of fornix deep brain stimulation in mild Alzheimer's disease. J Alzheimers Dis 2016;54(2):777–87.
[7] Braak H, Braak E. Staging of Alzheimer's disease-related neurofibrillary changes. Neurobiol Aging 1995;16(3):271–8. discussion 8-84.
[8] Hyman BT, Van Hoesen GW, Damasio AR, Barnes CL. Alzheimer's disease: cell-specific pathology isolates the hippocampal formation. Science 1984;225(4667):1168–70.
[9] Schultz RR, de Castro CC, Bertolucci PH. Memory with emotional content, brain amygdala and Alzheimer's disease. Acta Neurol Scand 2009;120(2):101–10.
[10] Seifan A, Marder KS, Mez J, Noble JM, Cortes EP, Vonsattel JP, et al. Hippocampal laminar distribution of tau relates to Alzheimer's disease and age of onset. J Alzheimers Dis 2015;43(1):315–24.
[11] Dunn KM, Nelson MT. Neurovascular signaling in the brain and the pathological consequences of hypertension. Am J Physiol Heart Circ Physiol 2014;306(1):H1–14.
[12] Greicius MD, Srivastava G, Reiss AL, Menon V. Default-mode network activity distinguishes Alzheimer's disease from healthy aging: evidence from functional MRI. Proc Natl Acad Sci U S A 2004;101(13):4637–42.
[13] Aggleton JP, Pralus A, Nelson AJ, Hornberger M. Thalamic pathology and memory loss in early Alzheimer's disease: moving the focus from the medial temporal lobe to Papez circuit. Brain 2016;139(Pt 7):1877–90.
[14] Papez JW. A proposed mechanism of emotion. Arch NeurPsych 1937;38(4):725–43.

[15] Aggleton JP, Brown MW. Episodic memory, amnesia, and the hippocampal-anterior thalamic axis. Behav Brain Sci 1999;22(3):425–44. discussion 44-89.
[16] Moscovitch M, Cabeza R, Winocur G, Nadel L. Episodic memory and beyond: the Hippocampus and neocortex in transformation. Annu Rev Psychol 2016;67:105–34.
[17] Squire LR, Genzel L, Wixted JT, Morris RG. Memory consolidation. Cold Spring Harb Perspect Biol 2015;7(8):a021766.
[18] DeFrance JF, Kitai ST, Shimono T. Electrophysiological analysis of the hippocampal-septal projections. I. Response and topographical characteristics. Exp Brain Res 1973;17(5):447–62.
[19] Luo AH, Tahsili-Fahadan P, Wise RA, Lupica CR, Aston-Jones G. Linking context with reward: a functional circuit from hippocampal CA3 to ventral tegmental area. Science 2011;333(6040):353–7.
[20] Swanson LW, Cowan WM. The connections of the septal region in the rat. J Comp Neurol 1979;186(4):621–55.
[21] Zaczek R, Hedreen JC, Coyle JT. Evidence for a hippocampal-septal glutamatergic pathway in the rat. Exp Neurol 1979;65(1):145–56.
[22] Orzel-Gryglewska J, Kusmierczak M, Majkutewicz I, Jurkowlaniec E. Induction of hippocampal theta rhythm by electrical stimulation of the ventral tegmental area and its loss after septum inactivation. Brain Res 2012;1436:51–67.
[23] Peterson GM. Differential projections to the hippocampus by neurons of the medial septum and vertical limb of the diagonal band. Brain Res 1994;646(1):129–34.
[24] Wyss JM, Swanson LW, Cowan WM. A study of subcortical afferents to the hippocampal formation in the rat. Neuroscience 1979;4(4):463–76.
[25] Lisman JE, Grace AA. The hippocampal-VTA loop: controlling the entry of information into long-term memory. Neuron 2005;46(5):703–13.
[26] Smith KS, Tindell AJ, Aldridge JW, Berridge KC. Ventral pallidum roles in reward and motivation. Behav Brain Res 2009;196(2):155–67.
[27] Fitch TE, Sahr RN, Eastwood BJ, Zhou FC, Yang CR. Dopamine D1/5 receptor modulation of firing rate and bidirectional theta burst firing in medial septal/vertical limb of diagonal band neurons in vivo. J Neurophysiol 2006;95(5):2808–20.
[28] Ito HT, Schuman EM. Frequency-dependent gating of synaptic transmission and plasticity by dopamine. Front Neural Circ 2007;1:1.
[29] Nazari-Serenjeh F, Rezayof A, Zarrindast MR. Functional correlation between GABAergic and dopaminergic systems of dorsal hippocampus and ventral tegmental area in passive avoidance learning in rats. Neuroscience 2011;196:104–14.
[30] Brocka M, Helbing C, Vincenz D, Scherf T, Montag D, Goldschmidt J, et al. Contributions of dopaminergic and non-dopaminergic neurons to VTA-stimulation induced neurovascular responses in brain reward circuits. Neuroimage 2018;177:88–97.
[31] Helbing C, Brocka M, Scherf T, Lippert MT, Angenstein F. The role of the mesolimbic dopamine system in the formation of blood-oxygen-level dependent responses in the medial prefrontal/anterior cingulate cortex during high-frequency stimulation of the rat perforant pathway. J Cerebr Blood Flow Metabol 2016;36(12):2177–93.
[32] Helbing C, Werner G, Angenstein F. Variations in the temporal pattern of perforant pathway stimulation control the activity in the mesolimbic pathway. Neuroimage 2013;64:43–60.
[33] Paxinos G, Watson C. The rat brain in stereotaxic coordinates. San Diego: Academic Press; 1988.
[34] Hennig J, Nauerth A, Friedburg H. RARE imaging: a fast imaging method for clinical MR. Magn Reson Med 1986;3:823–33.
[35] Angenstein F. The role of ongoing neuronal activity for baseline and stimulus-induced BOLD signals in the rat hippocampus. Neuroimage 2019;202:116082.
[36] Angenstein F. The role of ongoing neuronal activity for baseline and stimulus-induced BOLD signals in the rat hippocampus. Neuroimage 2019;202.116082–116082.
[37] Riemann S, Helbing C, Angenstein F. From unspecific to adjusted, how the BOLD response in the rat hippocampus develops during consecutive stimulations. J Cerebr Blood Flow Metabol 2017;37(2):590–604.
[38] Boeijinga PH, Mulder AB, Pennartz CM, Manshanden I, Lopes da Silva FH. Responses of the nucleus accumbens following fornix/fimbria stimulation in the rat. Identification and long-term potentiation of mono- and polysynaptic pathways. Neuroscience 1993;53(4):1049–58.
[39] DeFrance JF, Yoshihara H. Fimbria input to the nucleus accumbens septi. Brain Res 1975;90(1):159–63.
[40] Jas J, Almaguer W, Frey JU, Bergado J. Lesioning the fimbria-fornix impairs basolateral amygdala induced reinforcement of LTP in the dentate gyrus. Brain Res 2000;861(1):186–9.
[41] Blaha CD, Yang CR, Floresco SB, Barr AM, Phillips AG. Stimulation of the ventral subiculum of the hippocampus evokes glutamate receptor-mediated changes in dopamine efflux in the rat nucleus accumbens. Eur J Neurosci 1997;9(5):902–11.
[42] Ross EK, Kim JP, Settell ML, Han SR, Blaha CD, Min HK, et al. Fornix deep brain stimulation circuit effect is dependent on major excitatory transmission via the nucleus accumbens. Neuroimage 2016;128:138–48.
[43] Ferenczi EA, Zalocusky KA, Liston C, Grosenick L, Warden MR, Amatya D, et al. Prefrontal cortical regulation of brainwide circuit dynamics and reward-related behavior. Science 2016;351(6268):aac9698.
[44] Lohani S, Poplawsky AJ, Kim SG, Moghaddam B. Unexpected global impact of VTA dopamine neuron activation as measured by opto-fMRI. Mol Psychiatr 2016;22(4):585–94.
[45] Angenstein F, Krautwald K, Scheich H. The current functional state of local neuronal circuits controls the magnitude of a BOLD response to incoming stimuli. Neuroimage 2010;50(4):1364–75.
[46] Angenstein F. The actual intrinsic excitability of granular cells determines the ruling neurovascular coupling mechanism in the rat dentate gyrus. J Neurosci 2014;34(25):8529–45.
[47] Stypulkowski PH, Stanslaski SR, Giftakis JE. Modulation of hippocampal activity with fornix deep brain stimulation. Brain Stimul 2017;10(6):1125–32.
[48] Koubeissi MZ, Kahriman E, Syed TU, Miller J, Durand DM. Low-frequency electrical stimulation of a fiber tract in temporal lobe epilepsy. Ann Neurol 2013;74(2):223–31.
[49] Liu H, Temel Y, Boonstra J, Hescham S. The effect of fornix deep brain stimulation in brain diseases. Cell Mol Life Sci 2020. https://doi.org/10.1007/s00018-020-03456-4.
[50] Girault JA, Greengard P. The neurobiology of dopamine signaling. Arch Neurol 2004;61(5):641–4.
[51] Duzel E, Bunzeck N, Guitart-Masip M, Wittmann B, Schott BH, Tobler PN. Functional imaging of the human dopaminergic midbrain. Trends Neurosci 2009;32(6):321–8.
[52] Carr DB, Sesack SR. GABA-containing neurons in the rat ventral tegmental area project to the prefrontal cortex. Synapse (New York, NY) 2000;38(2):114–23.
[53] Fields HL, Hjelmstad GO, Margolis EB, Nicola SM. Ventral tegmental area neurons in learned appetitive behavior and positive reinforcement. Annu Rev Neurosci 2007;30:289–316.
[54] Hnasko TS, Hjelmstad GO, Fields HL, Edwards RH. Ventral tegmental area glutamate neurons: electrophysiological properties and projections. J Neurosci 2012;32(43):15076–85.
[55] Margolis EB, Lock H, Hjelmstad GO, Fields HL. The ventral tegmental area revisited: is there an electrophysiological marker for dopaminergic neurons? J Physiol 2006;577(Pt 3):907–24.
[56] Morales M, Root DH. Glutamate neurons within the midbrain dopamine regions. Neuroscience 2014;282:60–8.
[57] Van Bockstaele EJ, Pickel VM. GABA-containing neurons in the ventral tegmental area project to the nucleus accumbens in rat brain. Brain Res 1995;682(1–2):215–21.
[58] Yamaguchi T, Wang HL, Li X, Ng TH, Morales M. Mesocorticolimbic glutamatergic pathway. J Neurosci 2011;31(23):8476–90.
[59] Sulzer D, Joyce MP, Lin L, Geldwert D, Haber SN, Hattori T, et al. Dopamine neurons make glutamatergic synapses in vitro. J Neurosci 1998;18(12):4588–602.
[60] Krautwald K, Angenstein F. Low frequency stimulation of the perforant pathway generates anesthesia-specific variations in neural activity and BOLD responses in the rat dentate gyrus. J Cerebr Blood Flow Metabol 2011;32(2):291–305.
[61] Peeters RR, Tindemans I, De Schutter E, Van der Linden A. Comparing BOLD fMRI signal changes in the awake and anesthetized rat during electrical forepaw stimulation. Magn Reson Imaging 2001;19(6):821–6.
[62] Bick SK, Eskandar EN. Neuromodulation for restoring memory. Neurosurg Focus 2016;40(5):E5.
[63] Hardenacke K, Shubina E, Buhrle CP, Zapf A, Lenartz D, Klosterkotter J, et al. Deep brain stimulation as a tool for improving cognitive functioning in Alzheimer's dementia: a systematic review. Front Psychiatr 2013;4:159.
[64] Stone SS, Teixeira CM, Devito LM, Zaslavsky K, Josselyn SA, Lozano AM, et al. Stimulation of entorhinal cortex promotes adult neurogenesis and facilitates spatial memory. J Neurosci 2011;31(38):13469–84.
[65] Suthana N, Fried I. Deep brain stimulation for enhancement of learning and memory. Neuroimage 2014;85(Pt 3):996–1002.
[66] Xia F, Yiu A, Stone SSD, Oh S, Lozano AM, Josselyn SA, et al. Entorhinal cortical deep brain stimulation rescues memory deficits in both young and old mice genetically engineered to model Alzheimer's disease. Neuropsychopharmacology 2017;42(13):2493–503.